

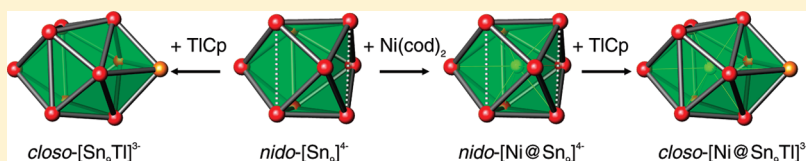
Addition of a Thallium Vertex to Empty and Centered Nine-Atom Deltahedral Zintl Ions of Germanium and Tin

Daniel Rios, Miriam M. Gillett-Kunnath, Jacob D. Taylor, Allen G. Oliver, and Slavi C. Sevov*

Department of Chemistry and Biochemistry, University of Notre Dame, Notre Dame, Indiana 46556, United States

S Supporting Information

ABSTRACT: Nickel atoms were inserted into nine-atom deltahedral Zintl ions of E_9^{4-} ($E = \text{Ge, Sn}$) via reactions with $\text{Ni}(\text{cod})_2$ ($\text{cod} = \text{cyclooctadiene}$), and $[\text{Ni}@\text{Sn}_9]^{3-}$ was structurally characterized. Both the empty and the Ni-centered clusters react with TlCp ($\text{Cp} = \text{cyclopentadienyl anion}$) and add a thallium vertex to form the deltahedral ten-atom *closo*-species $[\text{E}_9\text{Tl}]^{3-}$ and $[\text{Ni}@\text{E}_9\text{Tl}]^{3-}$, respectively. The structures of $[\text{Ge}_9\text{Tl}]^{3-}$ and $[\text{Ni}@\text{Sn}_9\text{Tl}]^{3-}$ showed that, as expected, the geometry of the ten-atom clusters is that of a bicapped square antiprism where the Tl-atom occupies one of the two capping vertices. This illustrates that centering a nine-atom cluster with a nickel atom does not change its reactivity toward TlCp . All compounds were characterized by electrospray mass spectrometry.



The structures of $[\text{Ge}_9\text{Tl}]^{3-}$ and $[\text{Ni}@\text{Sn}_9\text{Tl}]^{3-}$ showed that, as expected, the geometry of the ten-atom clusters is that of a bicapped square antiprism where the Tl-atom occupies one of the two capping vertices. This illustrates that centering a nine-atom cluster with a nickel atom does not change its reactivity toward TlCp . All compounds were characterized by electrospray mass spectrometry.

INTRODUCTION

For many years, the studies of nine-atom deltahedral Zintl clusters of Group 14 were directed mainly toward (a) improving their synthesis, (b) investigating the effects of various counteranions, and (c) understanding their electronic structures, geometric peculiarities, and deformations.¹ This changed when the first ligand-exchange reaction of Sn_9^{4-} with $(\text{mes})\text{Cr}(\text{CO})_3$ to form *closo*- $[\text{Sn}_9\text{Cr}(\text{CO})_3]^{4-}$ was reported by Eichhorn and Haushalter.^{2,3} A few years later, the first insertion of an atom inside the deltahedral cage of a Zintl cluster was carried out.⁴ Thus, Ge_9^{4-} clusters were reacted with $\text{Ni}(\text{CO})_2(\text{PPh}_3)_2$ in ethylenediamine at slightly elevated temperatures (35–45 °C) to produce the novel Ni-centered and Ni(PPh_3)-capped species $[\text{Ni}@\text{Ge}_9(\text{NiPPh}_3)]^{2-}$. At the time, these reactions were considered exotic and rare, but nowadays, such functionalizations and centering of clusters are widespread.⁵ Nonetheless, they led to a renaissance in the chemistry of deltahedral Zintl ions and ultimately to many new and exciting compounds. Thus, it is now known that these clusters can also oligomerize via oxidative coupling and can be functionalized with organic groups and a variety of main-group and transition-metal organometallic fragments.^{5b} However, while the chemistry of the empty clusters has been studied quite rigorously in recent years, not much is known about the reactivity of their centered counterparts and how similar or different they might behave toward various reagents. We have now undertaken such studies and report here our observations about the reactivity of empty and Ni-centered Ge_9 and Sn_9 clusters toward TlCp . They both add thallium atoms to form the corresponding *closo* ten-atom clusters $[\text{E}_9\text{Tl}]^{3-}$ and $[\text{Ni}@\text{E}_9\text{Tl}]^{3-}$, respectively ($E = \text{Ge, Sn}$). This similar reactivity suggests that the centered clusters might parallel the rich chemistry of the empty species in many other reactions as well.

RESULTS AND DISCUSSION

Thallium was added as the tenth vertex to both empty and Ni-centered nine-atom *nido*-clusters of germanium and tin by reactions of the clusters with TlCp in either ethylenediamine or pyridine in the presence of 2,2,2-crypt. The reactions with the empty clusters can be written simply as $\text{E}_9^{4-} + \text{TlCp} \rightarrow [\text{E}_9\text{Tl}]^{3-} + \text{Cp}^-$ for $E = \text{Ge, Sn}$. Both $[\text{Ge}_9\text{Tl}]^{3-}$ and $[\text{Sn}_9\text{Tl}]^{3-}$ can be clearly seen in the electrospray mass spectra of the reaction mixtures both as monoanions and ion-paired with one or two cations, but only the former was structurally characterized.

Single crystals of $[\text{K}(2,2,2\text{-crypt})]_3(\text{Ge}_9\text{Tl})\cdot 2\text{py}$ were obtained from pyridine solutions layered with toluene. The structure contains the ten-atom *closo*-cluster $[\text{Ge}_9\text{Tl}]^{3-}$ with the shape of a bicapped square antiprism where one of the capping vertices is the Tl-atom (Figure 1). The distances to the thallium cap, an average of 2.95 Å (range: 2.9049(5)–2.9969(6) Å), are naturally much longer than the distances at the germanium cap, an average of 2.58 Å (range: 2.5736(7)–2.5931(7) Å), because of the much larger size of the Tl-atom.⁶ In addition, the square capped by germanium is larger than the one capped by thallium with average Ge–Ge distances of 2.84 Å (range: 2.7907(7)–2.8690(7) Å) and 2.71 Å (range: 2.6971(7)–2.7300(7) Å) within the two squares, respectively. This suggests that the Ge-atoms of the larger square participate in good covalent interactions with all five germanium neighbors and are truly 5-coordinate, while the Ge-atoms of the smaller square interact with thallium much less strongly and behave more like 4-coordinate, just to their four germanium neighbors. Nonetheless,

Received: October 26, 2010

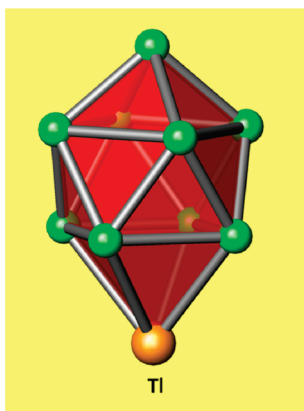


Figure 1. View of the *closo*-[Ge₉Tl]³⁻ cluster with the shape of a bicapped square antiprism where one of the caps is the thallium atom. The four Ge–Tl distances are 2.9049(5), 2.9058(6), 2.9921(5), and 2.9969(6) Å, while the Ge–Ge distances at the opposite Ge-cap are much shorter: 2.5736(7), 2.5845(7), 2.5863(7), and 2.5931(7) Å.

the thallium vertex is an integral part of the cluster as discussed in more detail for [Ni@Ge₉Tl]³⁻ below.

Not only the shape of [Ge₉Tl]³⁻ defines it as a *closo*-cluster but so do its charge and corresponding electron count. According to Wade–Mingos rules, a *closo*-cluster should have $4n + 2$ electrons, where n is the number of vertexes. This translates into 42 electrons for a ten-vertex cluster and, indeed, [Ge₉Tl]³⁻ has 9×4 (from 9 Ge-atoms) + 1×3 (from 1 Tl-atom) + 3 (from the charge) = 42 electrons. It should be pointed out that 20 of these electrons are predominantly lone pairs of electrons, one at each vertex of the cluster, while the remaining 22 are predominantly used for delocalized bonding within the cluster. By both shape and electron count, the cluster is closely related to the ten-atom species [E₉M(CO)₃]⁴⁻ (E = Sn, Pb; M = Cr, Mo, W),^{2,3,7} [E₉M–R]³⁻ (E = Si, Ge, Sn, Pb; M = Zn, Cd),⁸ [Sn₉Ir(cod)]³⁻,⁹ [Ge₉Cu(PR₃)₃]³⁻,¹⁰ and [E₁₀]²⁻ (E = Ge, Pb).¹¹

We note here that the structure of the tin-analogue [Sn₉Tl]³⁻ has already been reported and exhibits the same overall structure.¹² However, the synthetic approach used in that case is completely different from ours, namely, the heteroatomic cluster was crystallized directly from a ternary precursor with nominal composition “KTlSn” dissolved in ethylenediamine. The process of cluster formation in solution is not very clear because there is no evidence of pre-existing [Sn₉Tl]³⁻ clusters in the precursor. This is similar to the well-known but still mysterious process of generation of Sn₉⁴⁻ and Pb₉⁴⁻ clusters by dissolving Sn- or Pb-metal, respectively, in ethylenediamine solutions of alkali metals.¹³ In a similar manner, we recently obtained mixed [Ge_{9-x}Sn_x]ⁿ⁻ clusters by direct extraction from ternary precursors with a nominal composition “KGeSn”, although the same heteroatomic clusters could be made by mixing of the corresponding homoatomic species Ge₉⁴⁻ and Sn₉⁴⁻ in solvents with high dielectric constants such as DMSO, DMF, and acetonitrile.¹⁴

The aforementioned reported [Sn₉Tl]³⁻ cluster was structurally characterized in the compound [K(2,2,2-crypt)]₃ [(Sn₉Tl)_{0.5}(Sn₈Tl)_{0.5}]₂•2en and exhibited significant disorder.¹² It was modeled as an equimolar mixture of [Sn₉Tl]³⁻ and a nine-atom *closo*-[Sn₈Tl]³⁻ with $4n + 2 = 38$ electrons where $n = 9$. It is noteworthy to point out that the position of the Tl-atom in the latter is not the same as in the former. It actually replaces the

capping Sn-atom in [Sn₉Tl]³⁻, i.e., if we separate the two capping positions in [Sn₉Tl]³⁻ and write it as [Sn_{cap}–Sn₈–Tl_{cap}]³⁻, then the formula of the nine-atom species is [Tl_{cap}–Sn₈–empty_{cap}]³⁻. The details of this structure are important for the forthcoming discussion of the structure of the corresponding Ni-centered clusters [Ni@Sn₉Tl]³⁻.

We have already shown that Ge₉-clusters can be readily centered by reacting them with one equivalent of Ni(cod)₂.¹⁵ The simplicity of generating such species raises the question of how similar or different their chemistry is compared to the empty parent species. It turns out that in the particular case of the reaction with TlCp the empty and the Ni-centered Ge₉- and Sn₉-clusters behave in exactly the same way, i.e., they both produce Tl-capped ten-atom clusters. First, nickel atoms were inserted in empty germanium and tin clusters by the aforementioned reaction with Ni(cod)₂, and characterized structurally were the radical species with 3- charges [Ni@Ge₉]³⁻ and [Ni@Sn₉]³⁻. The existence of these Ni-centered radical clusters parallels directly the empty nine-atom clusters, which are often found with the 3- charge as E₉³⁻.¹ It should be pointed out that the central nickel atoms in the clusters behave as closed-shell d¹⁰ atoms that only participate in the cluster bonding but do not provide or take electrons.⁵ Thus, in terms of electron count, the Ni-centered clusters are isoelectronic with their empty counterparts as long as the charges are the same, i.e., [Ni@E₉]³⁻ and [E₉]³⁻ are isoelectronic (radicals) with 37 electrons each. The same is obviously valid for empty and Ni-centered Tl-capped ten-atom clusters. The radical nature of Sn₉³⁻ has already been shown by EPR,¹⁶ and although such measurements were not carried out for [Ni@E₉]³⁻ because of the lack pure samples (due to decomposition), similar radical behavior is expected for the centered clusters.

Here, we describe the structure of [Ni@Sn₉]³⁻ and compare it with the already reported [Ni@Ge₉]³⁻ as well as with the empty Sn₉³⁻ and Ge₉³⁻ clusters.^{15–17} Structurally characterized was the compound [K(2,2,2-crypt)]₆[Ni@Sn₉]₂•3en•tol with two crystallographically different [Ni@Sn₉]³⁻ clusters. As it happens, this compound is exactly isostructural with the reported analogous compound with empty Sn₉³⁻ clusters, namely [K(2,2,2-crypt)]₆[Sn₉]₂•1.5en•0.5tol (the solvent molecules in the latter were refined half occupied but are clearly fully occupied in the Ni-centered version),¹⁶ and the detailed and extensive description of the structure of the latter is valid here as well. One of the two independent clusters in both structures is disordered among two positions (shown in detail in the original publication¹⁶), but the second cluster is well behaved (Figure 2). The latter can be viewed as a distorted tricapped trigonal prism (Figure 2: atoms 1–5–7 and 2–6–8 form the trigonal bases of the prism while atoms 3, 4, and 9 are capping) with two elongated vertical edges (1–2 and 5–6 shown with broken lines). A comparison of the distances Sn–Sn and center–Sn (Ni–Sn for the centered cluster) in the empty and centered clusters shows clearly how the nickel insertion affects the metrics of the cluster. Overall, as can be expected, the cluster expands with some of the Sn–Sn distances increasing by as much as 0.3 Å, e.g., the elongated vertical edges 1–2 and 5–6 as well as the base edges 2–8 and 6–8 in the upper triangular base of the prism (see Figure 2 for distances). What is unexpected, however, is that the overall shape of the cluster changes from being somewhat compressed along the pseudo 3-fold axis when empty to almost perfectly spherical when centered. This is very clear from the radial distances from the center, which for the empty cluster fall

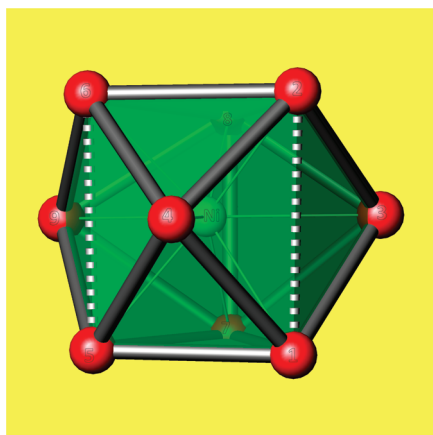


Figure 2. Ni-centered $[\text{Ni}@\text{Sn}_9]^{3-}$ with the shape of a distorted tricapped trigonal prism (the pseudo 3-fold axis is vertical; the two elongated vertical prismatic edges are shown with broken lines). Sn–Sn distances [Å] in $[\text{Sn}_9]^{3-}$ (from ref 16) and in $[\text{Ni}@\text{Sn}_9]^{3-}$ (in parentheses) between atoms 1–2: 3.501 (3.855); 1–3: 2.941 (3.035); 1–4: 2.955 (3.082); 1–5: 3.033 (2.977); 1–7: 3.098 (3.096); 2–3: 2.902 (2.985); 2–4: 2.938 (2.952); 2–6: 3.026 (3.131); 2–8: 3.089 (3.451); 3–7: 2.972 (3.021); 3–8: 2.964 (2.926); 4–5: 2.936 (3.062); 4–6: 2.977 (2.967); 5–6: 3.265 (3.738); 5–7: 3.133 (3.130); 5–9: 2.961 (2.983); 6–8: 3.134 (3.381); 6–9: 2.940 (2.992); 7–8: 3.194 (3.267); 7–9: 2.946 (3.018); and 8–9: 2.950 (2.915). Distances [Å] from the center in $[\text{Sn}_9]^{3-}$ and from Ni in $[\text{Ni}@\text{Sn}_9]^{3-}$ (in parentheses) to atoms: 1 – 2.482 (2.603); 2 – 2.440 (2.580); 3 – 2.748 (2.664); 4 – 2.771 (2.642); 5 – 2.408 (2.601); 6 – 2.419 (2.562); 7 – 2.421 (2.614); 8 – 2.440 (2.570); and 9 – 2.802 (2.743). The standard deviations for all distances are 0.002 and 0.001 Å in $[\text{Sn}_9]^{3-}$ and $[\text{Ni}@\text{Sn}_9]^{3-}$, respectively.

into two distinct ranges: shorter of around 2.4 Å to the six vertices of the trigonal prism and longer distances approaching 2.8 Å to the three capping atoms (see Figure 2 for individual distances). The Ni–Sn distances in the centered cluster, on the other hand, are all in a much narrower range of 2.562(1)–2.743(1) Å. In other words, the nickel insertion results in a cluster elongation along the pseudo 3-fold axis, while the capping atoms move inward closer to the center to achieve overall near spherical shape. One most likely reason for these differences comes simply from the different geometric requirements when arranging spheres in a cluster with or without a central sphere. In addition, similar Ni–Sn distances in the centered cluster mean optimized interactions of all nine tin atoms with the central atom. Such cluster expansion is also seen when going from the analogous empty germanium cluster Ge_9^{3-} to the centered $[\text{Ni}@\text{Ge}_9]^{3-}$.^{15,17} However, the metrics are not very clear in this case because of the great disorder in the latter, where $[\text{Ni}@\text{Ge}_9]^{3-}$ coexists with a Ni(en)-capped cluster $[\text{Ni}@\text{Ge}_9\text{Ni(en)}]^{3-}$.

As already mentioned, the Ni-centered clusters were next reacted with TlCp and produced the corresponding Ni-centered Tl-capped clusters $[\text{Ni}@\text{Ge}_9\text{Tl}]^{3-}$ and $[\text{Ni}@\text{Sn}_9\text{Tl}]^{3-}$. These clusters are clearly visible in the mass spectra of the reaction mixtures. Importantly, the spectrum of $[\text{Ni}@\text{(Ge}_9\text{Tl)}]^{3-}$, for example, shows only traces of uncapped clusters of $[\text{Ni}@\text{Ge}_9]$ (Supporting Information). This virtual absence of Tl-free clusters in the spectrum indicates that the thallium vertex is an integral part of the cluster and should not be treated simply as a Tl^+ cation. If thallium behaved as a cation, the spectrum would have shown a comparable or even stronger peak for the Tl^+ -free $[\text{Ni}@\text{Ge}_9]$ with respect to the Tl^+ -paired $[\text{Ni}@\text{(Ge}_9\text{Tl)}]$, just as

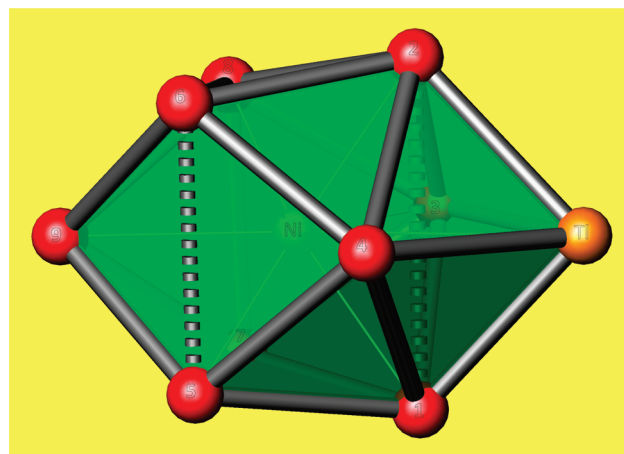


Figure 3. Ni-centered Tl-capped cluster $[\text{Ni}@\text{Sn}_9\text{Tl}]^{3-}$ with the shape of a square antiprism (atoms 1-to-8) capped by Sn9 (left) and Tl (right). Focusing on the Sn_9 -part, it is easy to see its resemblance of $[\text{Ni}@\text{Sn}_9]^{3-}$ (Figure 2) with the shape of a distorted tricapped trigonal prism. The range of Ni–Sn distances within the square antiprism, 2.582(1)–2.644(1) Å, is very similar to that in $[\text{Ni}@\text{Sn}_9]^{3-}$, 2.562(1)–2.664(1) Å, while the distance to the capping Sn9, 2.899(1) Å, is much longer than the Ni–Sn9 distance of 2.743(1) Å in $[\text{Ni}@\text{Sn}_9]^{3-}$. Distances from Tl to: Ni – 3.554(1), 1 – 2.975(1), 2 – 2.980(1), 3 – 3.215(1), and 4 – 3.155(1) Å.

the observed peak for the K^+ -free $[\text{Ni}@\text{(Ge}_9\text{Tl)}]^{3-}$ is stronger than that for the K^+ -paired $\{\text{K}[\text{Ni}@\text{(Ge}_9\text{Tl)}]\}^{3-}$. Attempted were further studies of the $[\text{Ni}@\text{(Sn}_9\text{Tl)}]^{3-}$ clusters in solution by ^{117/119}Sn NMR, but the samples did not produce clear and definite signals or any signal at all. The structure of the same anions was determined in the solid state in the compound $[\text{K}(2,2,2\text{-crypt})]_6\text{[}(\text{Ni}@\text{Sn}_9\text{Tl})_{0.52}(\text{Ni}@\text{Sn}_9)_{0.48}\text{]}\text{[}(\text{Ni}@\text{Sn}_9\text{Tl})_{0.36}(\text{Ni}@\text{Sn}_9)_{0.64}\text{]}\cdot 2\text{en}$. The complex structure contains two crystallographically different cluster sites one of which has the cluster disordered among two different orientations. On top of this, both cluster sites show coexisting Tl-capped and noncapped clusters $[\text{Ni}@\text{Sn}_9\text{Tl}]^{3-}$ (Figure 3) and $[\text{Ni}@\text{Sn}_9]^{3-}$, respectively. This coexistence is the same as in the reported $[\text{K}(2,2,2\text{-crypt})]_3\text{[}(\text{Sn}_9\text{Tl})_{0.5}(\text{Sn}_8\text{Tl})_{0.5}\text{]}\cdot 2\text{en}$ where the empty Tl-capped clusters $[\text{Sn}_9\text{Tl}]^{3-}$ coexist with noncapped nine-atom clusters $[\text{Sn}_8\text{Tl}]^{3-}$ at the same crystallographic site.¹² The only difference is that the noncapped clusters in the centered case are modeled as made of tin only, i.e., $[\text{Ni}@\text{Sn}_9]^{3-}$, instead of a centered heteroatomic $[\text{Ni}@\text{Sn}_8\text{Tl}]^{3-}$ that would correspond to $[\text{Sn}_8\text{Tl}]^{3-}$ in the empty-cluster case (discussed above). The absence of $[\text{Ni}@\text{Sn}_8\text{Tl}]^{3-}$ was confirmed by the mass spectrum of the reaction, which clearly shows predominantly $[\text{Ni}@\text{Sn}_9\text{Tl}]$ and $[\text{Ni}@\text{Sn}_9]$, both as monoanions and ion-paired with K^+ and $[\text{K}(2,2,2\text{-crypt})]^+$ (Figure 4).

The geometry of $[\text{Ni}@\text{Sn}_9\text{Tl}]^{3-}$ is best described as a bicapped square antiprism where Tl is one of the two capping atoms (Figure 3). The resemblance of its tin-only part to the centered homoatomic $[\text{Ni}@\text{Sn}_9]^{3-}$ (Figure 2) is very clear. The distorted tricapped trigonal prismatic shape of the latter, however, is even more distorted by further elongation of the prismatic edge of atoms 1–2 from 3.855(1) Å in $[\text{Ni}@\text{Sn}_9]^{3-}$ to 4.297(1) Å in $[\text{Ni}@\text{Sn}_9\text{Tl}]^{3-}$ as well as expansion of the pseudo square of atoms 1-to-4 upon capping it with Tl (average Sn–Sn distances of 3.01 Å in $[\text{Ni}@\text{Sn}_9]^{3-}$ but 3.14 Å in $[\text{Ni}@\text{Sn}_9\text{Tl}]^{3-}$). At the same time, the second elongated edge of atoms 5–6 in $[\text{Ni}@\text{Sn}_9]^{3-}$ is shortened from 3.738(1) to 3.553(1) Å in

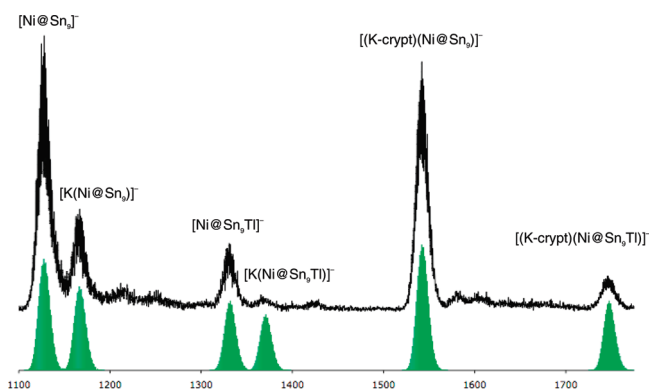


Figure 4. Section of the electrospray mass spectrum (in negative-ion mode; calculated peaks shown in green) of the reaction mixture that produced single crystals with $[\text{Ni}@\text{Sn}_9\text{Tl}]^{3-}$ and $[\text{Ni}@\text{Sn}_9]^{3-}$ occupying the same position in the structure. It is clear that species such as eventual $[\text{Ni}@\text{Sn}_8\text{Tl}]$ or $[\text{Sn}_8\text{Tl}]$ do not form in such a reaction.

$[\text{Ni}@\text{Sn}_9\text{Tl}]^{3-}$ and results in a much more regular Sn-capped square (atoms 5-to-8) in the latter. Lastly, a very noticeable change upon capping $[\text{Ni}@\text{Sn}_9]^{3-}$ with thallium is the shift of the Ni-atom away from Sn9 by about 0.16 Å (the Ni–Sn9 distances in $[\text{Ni}@\text{Sn}_9]^{3-}$ and $[\text{Ni}@\text{Sn}_9\text{Tl}]^{3-}$ are 2.743(1) and 2.899(1) Å, respectively). This can be interpreted as a result of either some Ni–Tl interactions or a secondary effect due to the opening of the Tl-capped square upon capping. Self-consistent Fenske–Hall calculations show that the HOMO of the cluster is virtually the lone pair of electrons at the Tl-vertex.¹⁸ However, despite the long Ni–Tl distance of 3.554(1) Å, that orbital shows also some small but nonzero contribution from the nickel's d_{z^2} .

We can also compare the metrics of the Ni-centered $[\text{Ni}@\text{Sn}_9\text{Tl}]^{3-}$ with its empty counterpart $[\text{Sn}_9\text{Tl}]^{3-}$,¹¹ although, because in both cases the clusters coexist with other species and are disordered, the comparison can not be very accurate. Nonetheless, small expansion of the cluster after the nickel insertion can be clearly seen. It is mainly noticeable within the Sn-capped square where the average Sn–Sn distance increases by 0.2 Å from 3.14 to 3.34 Å. This is quite understandable in light of the positioning of the central Ni-atom not exactly in the center of the whole $[\text{Sn}_9\text{Tl}]$ -cluster but rather in the center of the Sn-only part (the Ni–Sn9 and Ni–Tl distances are 2.899(1) and 3.554(1) Å, respectively). This makes it significantly closer to the square capped by Sn9 than to the opposite square capped by Tl and “pushes” the atoms of the former square outward and further from each other. Also, the Tl-capped squares in both $[\text{Sn}_9\text{Tl}]^{3-}$ and $[\text{Ni}@\text{Sn}_9\text{Tl}]^{3-}$ are noticeably puckered (butterfly like) resulting in two short and two long distances to the capping thallium: 3.093(4), 3.098(4), 3.118(3), and 3.164(4) Å in $[\text{Sn}_9\text{Tl}]^{3-}$ and 2.975(1), 2.980(1), 3.155(1), and 3.215(1) Å in $[\text{Ni}@\text{Sn}_9\text{Tl}]^{3-}$. The origin of the puckering of that square is yet another residual effect from the original tricapped trigonal prismatic shapes (distorted) of the parent noncapped clusters $[\text{Sn}_9]^{3-}$ and $[\text{Ni}@\text{Sn}_9]^{3-}$.

In conclusion, clearly the empty and Ni-centered nine-atom clusters of germanium and tin behave exactly the same with respect to reactions with TlCp. They both react and add a tenth Tl-vertex to form bicapped square antiprismatic *closo*-clusters of $[\text{E}_9\text{Tl}]^{3-}$ and $[\text{Ni}@\text{E}_9\text{Tl}]^{3-}$. It will be interesting to find whether this similar reactivity is confined only to this particular reaction or expands to more reactions of empty clusters with other organo-metallic compounds and organic halides and alkynes.

EXPERIMENTAL SECTION

All manipulations were carried out in a nitrogen-filled glovebox. Ethylenediamine (Alfa-Aesar, 99%) was distilled over sodium metal and stored in a gastight flask under nitrogen in the glovebox. The 2,2,2-crypt (4,7,13,16,21,24-hexaoxa-1,10-diazabicyclo[8.8.8]-hexacosane, Acros, 98%) and TlCp (thallium cyclopentadiene, Sigma-Aldrich, 97%) were used as received. Precursors of nominal compositions K_4Ge_9 and K_4Sn_9 were synthesized from stoichiometric mixtures of the elements (K, Strem, +99%; Ge and Sn, Alfa-Aesar, 99.999%) heated at 950 °C over 2 days in sealed niobium containers jacketed in evacuated fused silica tubes.

Synthesis and Crystallization of $[\text{K}(2,2,2\text{-crypt})]_3[\text{Ge}_9\text{-Tl}]_2\text{2py}$. A test tube was charged with a magnetic bar, 80 mg of K_4Ge_9 (0.099 mmol), 140 mg of 2,2,2-crypt (0.372 mmol), and 2 mL of pyridine. The mixture was stirred for 10 min making a dark red solution. A total of 27 mg of TlCp (0.100 mmol) and 20 mg of 2,2,2-crypt (0.053 mmol) were dissolved in 1.0 mL of pyridine in a separate test tube, and the solution was added dropwise to the first solution in a period of 30 min. Small amounts of black precipitate formed during the mixing. The resulting mixture was stirred for 2 h and then was centrifuged and filtered. ES-MS (m/z): 858 $[\text{Ge}_9\text{Tl}]^-$, 897 $[\text{K}(\text{Ge}_9\text{Tl})]^-$, 936 $[\text{K}_2(\text{Ge}_9\text{Tl})]^-$, and 1312 $[\text{K}(2,2,2\text{-crypt})(\text{Ge}_9\text{Tl})]^-$. The resulting dark solution was layered with toluene. After several weeks, red block crystals were present at the bottom of the test tube (ca. 65% crystalline yield). The analogous reaction with K_4Sn_9 produced the Tl-capped Sn_9 clusters $[\text{Sn}_9\text{Tl}]^{3-}$. ES-MS (m/z): 1273 $[\text{Sn}_9\text{Tl}]^-$, 1688 $[\text{K}(2,2,2\text{-crypt})(\text{Sn}_9\text{Tl})]^-$, and 2103 $[\text{K}(2,2,2\text{-crypt})_2(\text{Sn}_9\text{Tl})]^-$.

Synthesis and Crystallization of $[\text{K}(2,2,2\text{-crypt})]_6(\text{Ni}@\text{Sn}_9)_2\cdot 3\text{entol}$. A test tube was charged with a magnetic bar, 132 mg K_4Sn_9 (0.108 mmol), 122 mg 2,2,2-crypt (0.324 mmol), and 3 mL of ethylenediamine. The solution formed was initially a dark murky green color, but then changed to a dark black solution after stirring for several minutes. Then 27 mg of $\text{Ni}(\text{cod})_2$ (0.098 mmol) were added to the reaction mixture resulting in a green phase. The mixture was stirred for 2 h, after which it was centrifuged and filtered. ES-MS (m/z): 1128 $[\text{Ni}@\text{Sn}_9]^-$, 1167 $[\text{K}(\text{Ni}@\text{Sn}_9)]^-$, 1206 $[\text{K}_2(\text{Ni}@\text{Sn}_9)]^-$, 1543 $[\text{K}(2,2,2\text{-crypt})(\text{Ni}@\text{Sn}_9)]^-$, and 1582 $[\text{K}(\text{K}(2,2,2\text{-crypt})(\text{Ni}@\text{Sn}_9))]^-$. The resulting dark solution was then layered with toluene. After two weeks, dark brown-red crystals were observed at the bottom and along the sides of the test tube. The analogous reaction with K_4Ge_9 produced the Ni-centered clusters $[\text{Ni}@\text{Ge}_9]^{3-}$.¹⁵ ES-MS (m/z): 713 $[\text{Ni}@\text{Ge}_9]^-$, 752 $[\text{K}(\text{Ni}@\text{Ge}_9)]^-$, and 791 $[\text{K}_2(\text{Ni}@\text{Ge}_9)]^-$.

Synthesis and Crystallization of $[\text{K}(2,2,2\text{-crypt})]_6[(\text{Ni}@\text{Sn}_9\text{Tl})_x(\text{Ni}@\text{Sn}_9)_{(1-x)}]_2\cdot 2\text{en}$. A test tube was charged with a magnetic bar, 132 mg of K_4Sn_9 (0.099 mmol), 140 mg of 2,2,2-crypt (0.372 mmol), 27 mg of $\text{Ni}(\text{cod})_2$ (0.098 mmol), and 2 mL of ethylenediamine. The mixture was stirred for 10 min making a dark solution. A total of mg of TlCp (0.100 mmol) and 20 mg of 2,2,2-crypt (0.053 mmol) were dissolved in 1.0 mL of ethylenediamine in a separate test tube. This solution was added dropwise to the first solution over a period of 30 min. The resulting mixture was stirred for an additional 2 h and was then centrifuged and filtered. ES-MS (m/z): 1128 $[\text{Ni}@\text{Sn}_9]^-$, 1167 $[\text{K}(\text{Ni}@\text{Sn}_9)]^-$, 1332 $[\text{Ni}@\text{Sn}_9\text{Tl}]^-$, 1371 $[\text{K}(\text{Ni}@\text{Sn}_9\text{Tl})]^-$, 1543 $[\text{K}(2,2,2\text{-crypt})(\text{Ni}@\text{Sn}_9)]^-$, and 1747 $[\text{K}(2,2,2\text{-crypt})(\text{Ni}@\text{Sn}_9\text{Tl})]^-$. The resulting dark solution was layered with toluene. After two weeks, dark blocks were present at the bottom of the tube (ca. 55% crystalline yield). The analogous reaction with K_4Ge_9 produces the Ni-centered Tl-capped clusters $[\text{Ni}@\text{Ge}_9\text{Tl}]^{3-}$ according to the electrospray mass spectra. ES-MS (m/z): 713 $[\text{Ni}@\text{Ge}_9]^-$, 917 $[\text{Ni}@\text{Ge}_9\text{Tl}]^-$, 956 $[\text{K}(\text{Ni}@\text{Ge}_9\text{Tl})]^-$, and 995 $[\text{K}_2(\text{Ni}@\text{Ge}_9\text{Tl})]^-$.

Structure Determination. Single-crystal X-ray diffraction data were collected on a Bruker APEX diffractometer with a CCD area

Table 1. Selected Single-Crystal X-ray Diffraction Data Collection and Structure Refinement Parameters

compound	[K-crypt] ₃ [Ge ₉ Tl]•2py	[K-crypt] ₆ [(Ni@Sn ₉) ₂ •3en•tol	[K-crypt] ₆ [(Ni@Sn ₉ Tl) _x (Ni@Sn ₉) _(1-x)] ₂ •2en
fw	2262.64	5013.77	5046.4
space group, Z	P4 ₁ 2 ₁ 2, 8	P2 ₁ /c, 4	P2 ₁ /c, 4
a (Å)	21.9176(4)	28.0012(14)	28.2574(11)
b (Å)		23.3701(10)	23.4554(9)
c (Å)	36.9948(8)	27.6515(14)	27.7372(10)
β (°)	90	93.561(3)	93.236(1)
V (Å ³)	17771.6(6)	18059.9(15)	18354.6(12)
radiation, λ (Å)		Mo Kα, 0.71073	
ρ _{calc} (g cm ⁻³)	1.691	1.844	1.826
μ (mm ⁻¹)	5.007	2.846	3.561
R1/wR2, ^a I ≥ 2σ _I	0.0301, 0.0792	0.0575, 0.1414	0.0676, 0.1641
R1/wR2, ^a all data	0.0339, 0.0816	0.0907, 0.1542	0.0823, 0.1727

$${}^a R1 = [\sum ||F_o| - |F_c||] / \sum |F_o|; wR2 = \{[\sum w[(F_o)^2 - (F_c)^2]^2] / [\sum w(F_o)^2]\}^{1/2}; w = [\sigma^2(F_o)^2 + (AP)^2 + BP]^{-1}, \text{ where } P = [(F_o)^2 + 2(F_c)^2] / 3.$$

detector and K α radiation at 100 K. The structures were solved by direct methods and were refined on F² using the SHELXTL V5.1 package.¹⁹ Details of the data collection and structure refinements are given in Table 1.

Mass Spectrometry. Electrospray mass spectra (ES-MS) in negative-ion mode were recorded on a Micromass Quattro-LC triple quadrupole mass spectrometer (100 °C source temperature, 125 °C desolvation temperature, 2.0–2.8 kV capillary voltage, 25–45 V cone voltage). The samples were introduced by direct infusion with a Harvard syringe pump at 10 μ L/min.

ASSOCIATED CONTENT

Supporting Information. Electrospray mass spectrum of the reaction producing [Ni@Ge₉Tl] anions, clusters from Figures 1–3 drawn with anisotropic thermal ellipsoids, and X-ray crystallographic file of the structures in CIF format. This material is available free of charge via the Internet at <http://pubs.acs.org>.

AUTHOR INFORMATION

Corresponding Author

*ssevov@nd.edu.

ACKNOWLEDGMENT

We thank the National Science Foundation for the continuous financial support (CHE-0742365) and for the purchase of a Q-TOF electrospray mass spectrometer (CHE-0741793).

REFERENCES

- Reviews: (a) Corbett, J. D. *Chem. Rev.* **1985**, *85*, 383. (b) Corbett, J. D. *Struct. Bonding (Berlin)* **1997**, *87*, 157. (c) Fässler, T. F. *Coord. Chem. Rev.* **2001**, *215*, 347.
- Eichhorn, B. W.; Haushalter, R. C. *J. Am. Chem. Soc.* **1988**, *110*, 8704.
- (a) Eichhorn, B. W.; Haushalter, R. C. *J. Chem. Soc. Chem. Commun.* **1990**, 937. (b) Kesanli, B.; Fettinger, J.; Eichhorn, B. *Chem.—Eur. J.* **2001**, *7*, 5277.
- Initially the anion was reported as Ge-centered, i.e., [Ge@Ge₉Ni-PPh₃]²⁻ (Gardner, D. R.; Fettinger, J.; Eichhorn, B. *Angew. Chem., Int. Ed. Engl.* **1996**, *35*, 2852.), but was later corrected to [Ni@Ge₉Ni-PPh₃]²⁻ (Esenturk, E. N.; Fettinger, J.; Eichhorn, B. *Polyhedron* **2006**, *25*, 521.).
- Reviews: (a) Fässler, T. F.; Hoffmann, S. D. *Angew. Chem., Int. Ed.* **2004**, *43*, 6242. (b) Sevov, S. C.; Goicoechea, J. M. *Organometallics*

2006, *25*, 5678. (c) Sevov, S. C. In *Tin Chemistry: Fundamentals, Frontiers, and Applications*; Gielen, M.; Davies, A.; Pannell, K.; Tiekink, E., Eds.; Wiley-VCH: 2008; p 138. (d) Schrafe, S.; Fässler, T. F. *Phil. Trans. R. Soc. A* **2010**, *368*, 1265.

- Pyykkö, P.; Atsumi, M. *Chem.—Eur. J.* **2009**, *15*, 186.
- (a) Campbell, J.; Mercier, H. P. A.; Franke, H.; Santry, D. P.; Dixon, D. A.; Schrobilgen, G. J. *Inorg. Chem.* **2002**, *41*, 86. (b) Yong, L.; Hoffmann, S. D.; Fässler, T. F. *Eur. J. Inorg. Chem.* **2005**, 3663.
- (a) Goicoechea, J. M.; Sevov, S. C. *Organometallics* **2006**, *25*, 4530. (b) Zhou, B.; Denning, M. S.; Chapman, T. A. D.; Goicoechea, J. M. *Inorg. Chem.* **2009**, *48*, 2899. (c) Zhou, B.; Denning, M. S.; Jones, C.; Goicoechea, J. M. *Dalton Trans.* **2009**, 1571.
- (a) Downing, D. O.; Zavalij, P.; Eichhorn, B. W. *Eur. J. Inorg. Chem.* **2010**, 890. (b) Wang, J. Q.; Stegmaier, S.; Wahl, B.; Fässler, T. F. *Chem.—Eur. J.* **2010**, *16*, 1793.
- Schrafe, S.; Fässler, T. F. *Eur. J. Inorg. Chem.* **2010**, 1207.
- (a) Spiekermann, A.; Hoffmann, S. D.; Fässler, T. F. *Angew. Chem., Int. Ed.* **2006**, *45*, 3459. (b) Rios, D.; Sevov, S. C. *Inorg. Chem.* **2010**, *49*, 6396.
- Burns, R. C.; Corbett, J. D. *J. Am. Chem. Soc.* **1982**, *104*, 2804.
- Johannis, A. C. R. *Hebd. Seances Acad. Sci.* **1891**, *113*, 795.
- Gillett-Kunnath, M. M.; Petrov, L.; Sevov, S. C. *Inorg. Chem.* **2010**, *49*, 721.
- Goicoechea, J. M.; Sevov, S. C. *Angew. Chem., Int. Ed.* **2005**, *44*, 4026.
- Fässler, T. F.; Hunziker, M. Z. *Anorg. Allg. Chem.* **1996**, *622*, 837.
- Fässler, T. F.; Hunziker, M. *Inorg. Chem.* **1994**, *33*, 5380.
- (a) Hall, M. B.; Fenske, R. F. *Inorg. Chem.* **1972**, *11*, 768. (b) Manson, J.; Webster, C. E.; Pérez, L. M.; Hall, M. B. <http://www.chem.tamu.edu/jimp2/index.html>.
- Sheldrick, G. M. *SHELXTL*, version 5.1; Bruker-Nonius AXS: Madison, WI, 2001.